EPL, **137** (2022) 12005 doi: 10.1209/0295-5075/ac44e2 www.epljournal.org

Kink propagation in the Artificial Axon

XINYI QI and GIOVANNI ZOCCHI^(a)

Department of Physics and Astronomy, University of California - Los Angeles, CA, USA

received 24 August 2021; accepted in final form 20 December 2021 published online 12 April 2022

Abstract – The Artificial Axon is a unique synthetic system, based on biomolecular components, which supports action potentials. Here we consider, theoretically, the corresponding space extended system, and discuss the occurrence of solitary waves, or kinks. Such structures are indeed observed in living systems. In contrast to action potentials, stationary kinks are possible. We point out an analogy with the interface separating two condensed matter phases, though our kinks are always non-equilibrium, dissipative structures, even when stationary.

Copyright © 2022 EPLA

Introduction. – The Artificial Axon (AA) is a synthetic structure designed to support action potentials, thus generating these excitations for the first time outside the living cell. The system is based on the same microscopic mechanism as that operating in neurons, the basic components being: a phospholipid bilayer with embedded voltage gated ion channels, and an ionic gradient as the energy source, all in aqueous environment. Action potentials in real neurons are generated by the action of two opposite ionic gradients across the cell membrane, and two corresponding species of voltage gated ion channels. The rising edge of the action potential is produced by the opening of one channel species, and the falling edge by the opening of the other channel species. In the AA, there is only one ionic gradient and one channel species. The rising edge of the action potential is produced by the opening of the channels, the falling edge by channel inactivation. A current limited voltage clamp (CLVC) takes the role of the second ionic gradient [1,2].

More in detail, the physical AA [2] consists of a $\sim 100~\mu m$ size black lipid membrane with oriented, voltage gated potassium ion channels (KvAP) embedded in it. The membrane separates two compartments ("in" and "out") where different KCl concentrations are maintained, resulting in an equilibrium (Nernst) potential $V_N \sim +40~{\rm mV}$, referring voltages to the grounded "outside". Connection to the electronics for sensing and control are through AgCl electrodes. The specific ion channel used in [2] was the KvAP, a bacterial channel from the thermophilic archaea Aeropyrum pernix [3]. KvAP was the first voltage gated ion channel of which the structure was determined to atomic resolution [4,5]. The channel opens at positive

voltages, and is closed at voltages below $\sim -50\,\mathrm{mV}$; however its dynamics is complex, involving also an "inactive" state [6].

In the experiments, the AA is held off equilibrium, at a negative "resting potential" $V_r \sim -100\,\mathrm{mV}$, by a Current Limited Voltage Clamp (CLVC) connected to the inside chamber. This device is a regular voltage clamp (a "zero output impedence" voltage source) in series with a large resistance R_c . Its effect is to inject a current $I_c = [V_c - V(t)]/R_c$ into the AA, where $(1/R_c)$ is the clamp conductance, V_c the clamp voltage, V(t) the membrane potential (the axon voltage). Thus the CLVC has the same effect as a second ionic gradient with corresponding Nernst potential V_c and total leak conductance $(1/R_c)$. It allows to keep the system at an off-equilibrium "resting potential", without actually clamping the voltage, and thus allowing voltage dynamics, specifically action potential firing.

As a dynamical system for the voltage, the AA operates in zero space dimensions (similar to the "space clamp" setup with real axons [7,8]). That is, each side of the membrane is basically an equi-potential surface (the name Artificial Axon, while a misnomer in this respect, is historical [1] and we propose to keep it for the original and future versions). Inspired by this system, here we consider —theoretically— the corresponding space extended dynamical system. We focus on the existence of solitary wave solutions, or propagating kinks (we will use the two terms interchangeably, to mean a front which propagates keeping its shape).

Kinks appear in many areas of condensed matter physics [9], from domain walls in magnetic materials [10,11] to pattern forming chemical reactions [12]. We arrived at our particular nonlinear structures through

 $^{^{(}a)}E$ -mail: zocchi@physics.ucla.edu (corresponding author)

the AA, however, these same fronts have been analyzed theoretically and produced experimentally before. In a neuroscience setting, Loewenstein and Sompolinsky [13] discussed theoretically calcium wavefronts propagating in single neurons, in the context of neuronal temporal integration. These wavefronts are our same kinks, as the underlying reaction-diffusion equation is basically the same. In their model, they show how a space pattern of resting potentials may arise within a single neuron, due to the existence of these fronts. The voltage pattern may in turn generate graded, persistent firing. Thus in their study the presence of kinks allows to generate memory within single neurons, and the neuronal temporal integration necessary for basic psychomotorial functions such as posture control.

Calcium waves are indeed a general mechanism of inter-cellular signaling, and have been studied accordingly [14,15]. In particular, in the nervous system they represent a form of non-synaptic communication for instance between glial cells [14,16].

In the context of electrophysiological pattern formation in confluent cell cultures, McNamara et al. [17] discuss the emergence of spatial domains of different resting potential, separated by domain walls, which are again the same kinks. Their analysis of domain walls is basically the same as we present here; in their cell-based experimental system they observe directly the spatial structure of the kinks and their motion. Their study pinpoints the relevance of these structures to pattern formation in tissue, not least during embryogenesis.

The aforementioned examples signify that kinks are important structures both in living and inanimate matter. With the Artificial Axon we wish to develop a cell-free system where similar phenomena could be studied, perhaps under more easily controlled conditions, and new pattern forming systems envisaged.

We show the existence of travelling kinks in our system, and study numerically their characteristics in relation to the control parameters, which are the command voltage and the conductance of the CLVC. Then we discuss a "normal form" for this class of dynamical systems, highlighting the relation with other kinks separating two condensed matter phases, such as the nematic-isotropic interface in liquid crystals. The nonlinearities which thus arise retrace the development of simplified models of the Hodgkin-Huxley axon [18], such as introduced 60 years ago by Fitzhugh [19] and Nagumo et al. [20]. Looking at kinks thus provides a somewhat different perspective on a classic topic in the study of excitable media.

Results. – We consider the AA in one space dimension. The physical system we have in mind is a \sim 1 cm long, \sim 100 μ m wide supported strip of lipid bilayer with one species of voltage gated ion channels embedded (fig. 1). The bilayer might be anchored to the solid surface so as to leave a sub-micron gap (the "inside" of the axon) in between. At present, the stability of the bilayer stands in

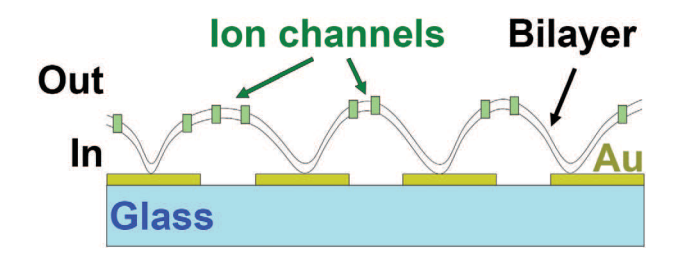


Fig. 1: Schematic drawing of a possible experimental realization of the space extended AA (not to scale). The phospholipid bilayer with embedded K^+ ion channels is chemically anchored, in spots, to a patterned $\sim 5\,\mathrm{nm}$ thick Au layer. A continuous AgCl electrode (not shown) is also deposited on the slide, providing the connection to the CLVC. The "outside" compartment is grounded through an electrode "at infinity" (not shown). The outside has a large concentration of KCl relative to the inside.

the way of a practical realization, but this problem is not unsurmountable.

The bilayer acting essentially like the dielectric in a parallel plates capacitance, the local charge density is related to the voltage by $(\partial/\partial t)\rho(x,t)=c\,(\partial/\partial t)V(x,t)$ where c and ρ are capacitance and charge per unit length, respectively. The current inside the axon follows Ohm's law: $j=-(1/r)(\partial V/\partial x)$, where r is the resistance per unit length; then charge conservation leads to the diffusion equation for the potential: $(\partial V(x,t)/\partial t)-(1/(rc))(\partial^2 V(x,t)/\partial x^2)=0$.

In the AA, the gradient of K⁺ ions across the membrane results in an equilibrium (Nernst) potential $V_N =$ $(T/|e|) \ln([K^+]_{out}/[K^+]_{in});$ here T is the absolute temperature in energy units, and e the electronic charge; square brackets denote concentration. However, the "resting" system is held at an off-equilibrium voltage by the current injected through a current limited voltage clamp (CLVC) [1]. The active elements in the system are voltage gated potassium channels inserted in the membrane: these are molecular pores which, in the open state, selectively conduct K⁺ ions. The KvAP channel used in [2,21] has three functionally distinct states: open, closed, and inactive; the presence of the inactive state allows the system to generate action potentials. Here we consider the simpler case of a "fast" channel with no inactivation. Then the channels can be described by an equilibrium function $P_O(V)$ which gives the probability that the channel is open if the local voltage is V. For the KvAP, the function $P_O(V)$ is well described by a Fermi-Dirac distribution [22].

Introducing the current sources in the diffusion equation above one arrives at the following (1+1)D dynamical system:

$$\frac{\partial V(x,t)}{\partial t} - \frac{1}{rc} \frac{\partial^2 V}{\partial x^2} = \frac{\chi}{c} P_O(V) [V_N - V(x,t)] + \frac{\chi_c}{c} [V_c - V(x,t)]. \tag{1}$$

V is the voltage inside the axon (referred to the grounded outside), and we assume a distributed "space clamp" for the CLVC (this would be provided by an electrode along the axon). Equation (1) is of the general form of a reactiondiffusion system; these are usually studied in the context of pattern forming chemical reactions. For us it represents a continuum limit, i.e., we consider a uniform, distributed channel conductance instead of discrete, point-like ion channels. This is a mean field approximation which neglects correlations between nearby channels. The first term on the RHS of (1), when multiplied by c, is the channel current, proportional to the driving force $(V_N - V)$; V_N is the Nernst potential, χ the conductance (per unit length) with channels open (i.e., $\chi = n\chi_0$, χ_0 single channel conductance, n number of channels per unit length). The second term is the current injected by the clamp; V_c is the clamp voltage (which is a control parameter in the experiments), χ_c the clamp conductance (per unit length), which is a second control parameter. The function $P_O(V)$ is a Fermi-Dirac distribution:

$$P_O(V) = \frac{1}{\exp[-q(V - V_0)/T] + 1},$$
 (2)

where q is an effective (positive) gating charge and V_0 the midpoint voltage where $P_O(V_0) = 1/2$.

To fix ideas, we will use parameters consistent with the AA in [21]: $V_N = 50\,\mathrm{mV},\ \chi/c = 100\,\mathrm{s}^{-1},\ \chi_c/c = 5\,\mathrm{s}^{-1},\ (1/rc) = 1\,\mathrm{cm}^2/\mathrm{s},\ V_0 = -10\,\mathrm{mV},\ q/T = 0.08\,\mathrm{(mV)}^{-1}.$ We use Gaussian units except that we express voltages in mV: this is more convenient to relate to experimental systems. Also, the temperature in (2) and elsewhere is in energy units; thus at room temperature $T/|e| \approx 25\,\mathrm{mV}$, where e is the charge of the electron.

The possibility of travelling kink solutions of (1) and (2) arises because, with the clamp at a negative voltage, say $V_c = -100 \,\mathrm{mV}$, there exist two stable fixed points of (1) (uniform, time-independent solutions). One fixed point, call it V_1 , is close to the Nernst potential, with channels essentially open $(P_O(V_1) \approx 1)$; it is given approximately by $V_1 \approx (\chi V_N + \chi_c V_c)/(\chi + \chi_c)$. The other stable fixed point (call it V_3) is close to the clamp voltage $(V_3 \approx V_c)$, with channels essentially closed $(P_O(V_3) \approx 0)$. A stable kink solution exists, asymptotically connecting these two stable fixed points (a third fixed point is unstable and will be discussed later). Exact values for V_1 and V_2 are found by solving numerically the corresponding algebraic equation.

The essential parameters in (1) are the diffusion constant $D \equiv 1/(rc)$ and χ/c ; from these we can form a characteristic length scale $\Delta = 1/\sqrt{r\chi}$ which gives the scale of the width of the kink solution, and a characteristic velocity $v = D/\Delta = (1/c)\sqrt{\chi/r}$ which similarly gives the scale for the kink velocity. With the parameters above, $\Delta \approx 1\,\mathrm{mm}$ and $v \approx 10\,\mathrm{cm/s}$.

Figure 2 shows snapshots of a travelling kink obtained by integrating (1), (2) using the parameters above and $V_c = -200 \,\mathrm{mV}$. The kink was launched with a hyperbolic

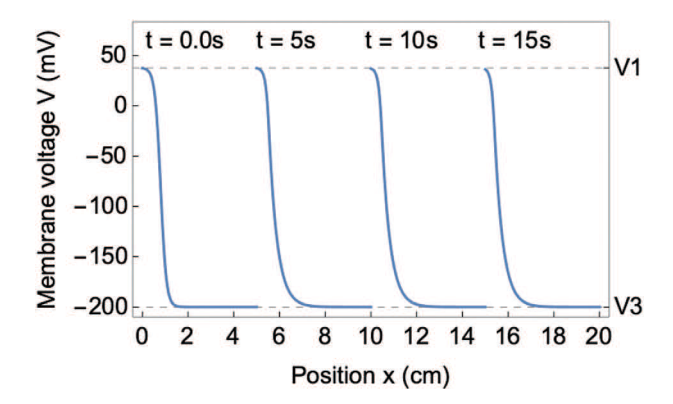


Fig. 2: The traveling kink solution V(x,t) for (1), (2). The plot shows snapshots of the kink at different times; the initial condition (t=0) is a hyperbolic tangent. Parameter values are those given in the text, with a clamp voltage $V_c = -200 \,\mathrm{mV}$. The dotted horizontal lines show the fixed points V_1 and V_3 . Notice that the shape of the kink shifts from the initial condition at $t=0.0 \,\mathrm{s}$ to a stable shape afterwards.

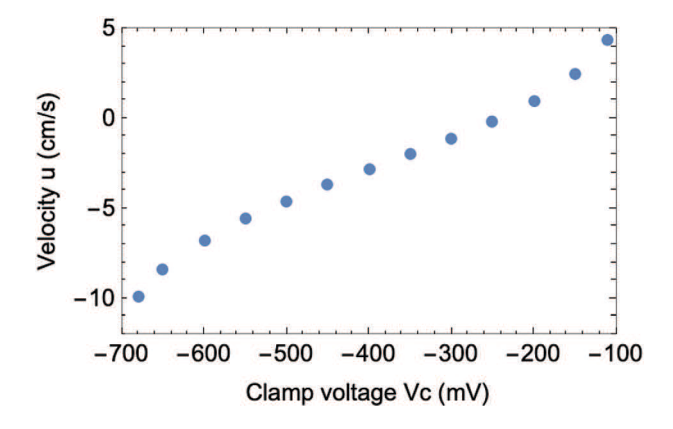


Fig. 3: Plot of kink velocity vs. clamp voltage. Parameter values are those given in the text. The velocity is determined by tracking the minimum of the first derivative of V(x,t), which corresponds to the inection point of the kink-shaped wavefront. The leftmost and rightmost data points are close to the values of V_c beyond which the kink solution disappears. The graph is asymmetric with respect to right moving and left moving kinks.

tangent initial condition (t = 0 trace in fig. 2); it is found to quickly (on a time scale $\sim c/\chi$) attain a stable limiting shape and thereafter travel at constant velocity. The velocity depends on the clamp voltage V_c , as shown in fig. 3. We measure it by tracking the inflection point of the solution V(x,t). The solitary wave solution exists only for V_c within certain bounds; correspondingly there is a maximum velocity of the kink, while the minimum velocity is zero, as we show below.

Let us now analyze these solitary wave solutions (see, e.g., [9]). Equation (1) is of the form

$$\frac{\partial V(x,t)}{\partial t} - \frac{\partial^2 V}{\partial x^2} = g(V), \tag{3}$$

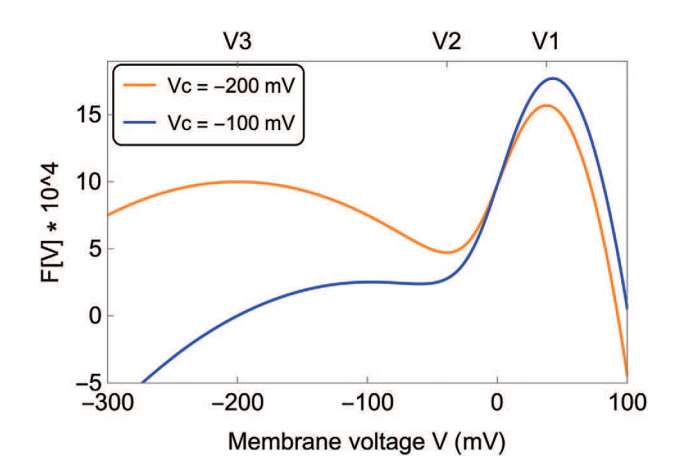


Fig. 4: The function $F(\varphi)$ obtained from (4) vs. the (dimensional) membrane voltage, for clamp voltages of $-100\,\mathrm{mV}$ and $-200\,\mathrm{mV}$. Parameters are as given in the text. The fixed points $V_1,\,V_2,\,V_3$ shown refer to the yellow ($V_C=-200\,\mathrm{mV}$) curve. As V_C is decreased below $-200\,\mathrm{mV}$ the global maximum becomes the secondary maximum and vice-versa. Increasing V_c above $-100\,\mathrm{mV}$, the secondary maximum eventually disappears, at which point there is no kink solution.

where we have changed to non-dimensional variables using $\Delta = 1/\sqrt{r\chi}$, $\tau = c/\chi$, V_N as the units of length, time, and potential, respectively. Then,

$$\begin{cases}
g(V) = P_O(V)[1 - V] + \frac{\chi_c}{\chi} \left[\frac{V_c}{V_N} - V \right], \\
P_O(V) = \left\{ \exp \left[-\frac{qV_N}{T} \left(V - \frac{V_0}{V_N} \right) \right] + 1 \right\}^{-1}.
\end{cases} (4)$$

From (3) and (4) we see that the control parameters of this system are indeed the clamp conductance (more precisely, the ratio χ_c/χ) and the clamp voltage (the ratio V_c/V_N); the parameters which describe the channels, *i.e.*, q and V_0 in (4), are not easily varied experimentally, so we consider them fixed. We look for a travelling wave solution: $V(x,t) = \varphi(x-ut) = \varphi(z), z \equiv x-ut$; then from (3)

$$\varphi'' + u \varphi' = -\frac{\mathrm{d}}{\mathrm{d}\varphi} F(\varphi),$$
 (5)

where F is the primitive of g, i.e., $g(\varphi) = \mathrm{d}F/\mathrm{d}\varphi$. We may interpret (5) as the equation of motion of a unit mass in a potential energy F, subject to a frictional force proportional to the velocity. The dissipation parameter u is the velocity of the kink. In fig. 4 we plot the function F obtained from integrating g in (4); the analytic expression, which involves the poly log function, is readily obtained with Mathematica.

The kink solution displayed in fig. 2 corresponds, in terms of eq. (5) and fig. 4, to the particle (of coordinate φ) starting with zero velocity at the maximum $\varphi = V_1$ and arriving (after an infinite time) at the secondary maximum $\varphi = V_3$, also with zero velocity. The value of the dissipation parameter u for which this is possible corresponds

to the propagation velocity of the kink. Different velocities are possible transiently, for example, a kink initially steeper than the asymptotic shape will initially travel faster, and slow down as it attains the stable shape and velocity. This "shaping" of the signal expresses the existence of a stable, unique solitary wave solution. It motivated the electronic realization of an axon, and the corresponding influential dynamical system model, by Nagumo et al. [20].

Varying the clamp voltage V_c modifies the potential F, and the kink velocity u changes correspondingly, as shown in fig. 3. For increasing V_c , the difference $F(V_1) - F(V_3)$ increases, while the secondary maximum at $V = V_3$ becomes less pronounced (fig. 4). Correspondingly, the kink velocity increases. At a critical clamp value $V_c \approx -92.8 \,\mathrm{mV}$ the secondary maximum disappears (the minimum at V_2 becomes an inflection point, then reverses curvature), so no kink solution exists for higher clamp voltages. Conversely, as V_c is decreased, the difference $F(V_1) - F(V_3)$ decreases, goes through zero and becomes negative. Correspondingly the kink velocity also goes through zero and then reverses sign. In short, $F(V_1) - F(V_3)$ increases monotonically with increasing V_c , as does the kink velocity u. There is a maximum positive velocity and a maximum negative velocity (the two are not the same). There is a particular clamp voltage ($V_c \approx -244.0 \,\mathrm{mV}$ with our parameters) such that the kink is stationary (u = 0). Trivially, for each rightmoving kink there is an identical mirror-image left-moving kink, if one inverts the boundary conditions at infinity. The asymmetry of the curve of the velocity (u) vs. clamp voltage (V_c) with respect to u = 0 (fig. 3) is a consequence of the behavior of the function F(V) as the parameter V_c is varied (fig. 4). Namely, if $V_c^{(0)}$ is the clamp value such that u=0, then the two functions F(V) for parameter values $V_c^{(0)} \pm \Delta V_c$ are not related by the mirror symmetry that would translate into the velocity curve being symmetric around u = 0.

From fig. 4 we also see that two more kink solutions exist, one connecting the maximum at V_1 with the minimum at V_2 (evidently travelling at a faster speed compared to the kink connecting V_1 and V_3), and a third one connecting V_3 and V_2 . These solutions are linearly unstable, because the fixed point at V_2 is unstable; thus they would not be observed experimentally. However, they can still be "observed" numerically, as we see below.

It is interesting to put this problem in a "normal form", and see the connection to other kinks in condensed matter physics. The simplest function F in (5) which supports a kink solution of (3) has a maximum and a minimum, *i.e.*, a cubic nonlinearity. A kink solution exists connecting the maximum and the minimum, but it is unstable as the minimum is an unstable fixed point. The next simplest case is that F has three extrema (two maxima and a minimum); assuming a single control parameter, we may write

$$F(V) = a \left[2(1 - \alpha)V^2 + \frac{4}{3}\alpha V^3 - V^4 \right], \tag{6}$$

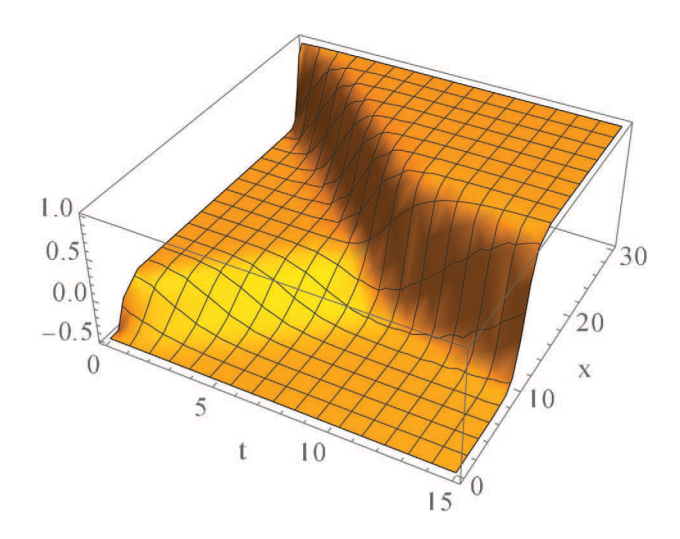


Fig. 5: A 3D plot showing the collision of two different kinks. They are obtained integrating (7) with a=0.5, $\alpha=0.5$, and appropriate initial conditions. Notice the velocity change after the collision. However, these kinks are linearly unstable and so would not be observed experimentally.

 $a > 0, \alpha \le 1$, where we put one stable fixed point at $V_1 = 1$ and the unstable fixed point (the minimum of F) at $V_2 = 0$. The third (stable) fixed point is at $V_3 = (\alpha - 1)$. This is not the most general form: the choice $V_2 = 0$ forces F to be an even function at the "coexistence point" $\alpha = 0$, as we discuss below; however, this choice allows to discuss unstable kink solutions also. Apart from this difference, this situation corresponds to (4); the parameter α has the role of V_c/V_N , if χ_c/χ is fixed. Plots of F(V) from (6) evolve, varying α , in a similar way to the plots shown in fig. 4 for varying V_c . For $-1 < \alpha \le 1$ a stable kink with $V(x \to -\infty) = V_1$ and $V(x \to +\infty) = V_3$ exists, travelling with a speed u which increases monotonically with increasing α . The stationary kink is obtained for $\alpha = 0$; for $\alpha > 0$ the kink travels to the right and for $\alpha < 0$ to the left. The simplest stable kink is thus a solution of

$$\frac{\partial V(x,t)}{\partial t} - \frac{\partial^2 V}{\partial x^2} = 4a[(1-\alpha)V + \alpha V^2 - V^3]. \quad (7)$$

The cubic nonlinearity in this equation is a feature of several reduced parameters models of nerve excitability, notably Fitzhugh's "BVP model" [19], and indeed of the original Van der Pol relaxation oscillator [23], in appropriate coordinates. Two further kink solutions of (7) exist, connecting V_1 and V_2 , and V_3 and V_2 . These are linearly unstable, but they can still be obtained numerically, with the trick of arranging for the unstable fixed point to be at V=0, as we did in (6). In this way, one can even discuss collisions between different kinks: the only non-trivial example stemming from (6) is shown in fig. 5.

Namely, the kink connecting V_1 and V_2 collides with the kink connecting V_3 and V_2 travelling in the opposite direction, resulting in the stable kink connecting V_1 and V_3 in the final state.

To recapitulate: the fixed points of (3) are uniform, time-independent solutions which we might call "phases". Two different phases can be connected by a kink. The fixed points are zeros of g, i.e., extrema of F, but the stable fixed points are maxima of F while the unstable ones are minima. For the purpose of classifying, F is analogous to minus the free energy of a Landau theory describing a corresponding phase transition. The stationary kink $(\alpha = 0 \text{ in } (6))$ is the interface separating two coexisting phases. For $\alpha \neq 0$, one of the two phases is more stable and grows at the expense of the other (i.e., the kink moves). However, we must remember that our system is never in thermodynamic equilibrium. Even when the kink is stationary, there are macroscopic currents in the system (the clamp current and the channels current), and detailed balance is violated.

The function F derived from (4), which is shown in fig. 4, has the same general form as (minus) the mean field free energy which describes the nematic-isotropic transition in liquid crystals [9], or also the liquid-gas transition. For the former, and following the notation in [9], the free energy f as a function of the order parameter S is

$$f = \frac{1}{2}a(T - T^*)S^2 - wS^3 + uS^4,$$
 (8)

where $S = P_2(\cos \theta)$, P_2 is the Legendre Polynomial of order 2 and θ the angle between the molecular axis and the director vector. For fixed V_c , the evolution of -F for varying χ_c/χ (where F is the primitive of (4)) mirrors the evolution of (8) for varying temperature T. Namely, for small values of χ_c/χ there is a global minimum at positive V (i.e., channels essentially open) and a secondary minimum at negative V (channels essentially closed). Increasing χ_c/χ one reaches a coexistence point where -Fhas the same value at the two minima, after which the global minimum is at negative V and the secondary minimum at positive V (fig. 4), i.e., the stable phase is with channels essentially closed. As in (8) there are limits of meta-stability where the secondary minimum disappears. If we allow V_c as a second control parameter, we find a coexistence line in the V_c - χ_c/χ plane ending in a critical point, i.e., the phenomenology of a liquid-gas transition. For parameter values on the coexistence line, the kink is stationary.

For the case of the stationary kink, one can write an implicit formula for the shape: with u=0, multiplying (5) by φ' and integrating from $-\infty$ to x, with the boundary conditions $\varphi' \to 0$, $\varphi \to \varphi_1$ for $x \to -\infty$ one finds

$$\frac{\mathrm{d}\varphi}{\sqrt{-F(\varphi) + F(\varphi_1)}} = -\sqrt{2}\mathrm{d}x. \tag{9}$$

For the stationary kink of (7), which occurs for $\alpha = 0$, we have $F(\varphi) = a(2\varphi^2 - \varphi^4)$, the maxima of F are at $\varphi = \pm 1$, and integrating (9) we find $\varphi(x) = \tanh(-\sqrt{2ax})$. This is the same kink as in the mean field theory of the Ising ferromagnet, separating two domains of opposite magnetization [9]. It has a special symmetry (inversion about its

center), stemming from the symmetry of this particular F, which is an even function at the coexistence point $\alpha=0$. The function F derived for the Artificial Axon from (4) has no such symmetry, and correspondingly the stationary kink is not inversion symmetric about its center, as fig. 2 shows. For this kink too an analytic expression can be obtained from (9) in terms of special functions.

Conclusions. - We have discussed the occurrence of travelling kink solutions in a dynamical system which represents a space extended Artificial Axon. We considered the simplest limit: "fast" channels described by an equilibrium opening probability $P_O(V)$, and no inactivation. Even so, the velocity of the kink represents a non trivial eigenvalue problem, expressed by (5). More generally, introducing channel dynamics increases the dimensionality of the dynamical system and leads to more structure (oscillations, limit cycles, *i.e.*, action potentials) as is well known. We point out a connection to similar kinks in other areas of condensed matter physics: some questions which can be asked of these systems are similar, for instance, effects beyond mean field [10,24]. For us, this means replacing the uniform channel conductance with a space distribution of point-like channels, eventually interacting, eventually mobile. Introducing channel dynamics (see, e.g., [25,26]), it may be interesting to extend this study to pattern formation in 2 space dimensions. McNamara et al. [17] indeed present an experimental realization of such a system, with living cells. Their experimental system consists of gap-junction coupled, cultured cells. They use a cell line engineered to express a K⁺ channel and channel rhodopsin, the latter providing a light-actuated control parameter akin to the CLVC conductance in the AA. Using a voltage sensitive dye for the measurements, they observe bistability of their system in a region of parameter space, thus patches of tissue at different resting potential, separated by domain walls (kinks) which can be stationary or moving. They go on to show that differentiating myoblasts exhibit collective domain wall migration during myogenesis (the formation of muscle tissue). Their results reaffirm the importance of electrophysiological pattern formation, mediated by domain wall drift, for embryogenesis. An electrophysiologically equivalent, synthetic system could in principle be constructed with the present physical AAs. Namely, an array of (zero space dimension) AAs with nearest neighbor connections through large resistors, would presumably support similar voltage patterns. In this way, systems built on AAs could be developed into cell-free breadboards for electrophysiology research. In general, this approach may inspire the construction of new reaction-diffusion systems [27] with interesting spatio-temporal dynamics.

* * *

This work was supported by NSF grant DMR - 1809381.

REFERENCES

- [1] ARIYARATNE A. and ZOCCHI G., J. Phys. Chem. B, **120** (2016) 6255.
- [2] VASQUEZ H. G. and ZOCCHI G., EPL, 119 (2017) 48003.
- [3] RUTA V., JIANG Y., LEE A., CHEN J. and MACKINNON R., *Nature*, **422** (2003) 180.
- [4] JIANG Y., LEE A., CHEN J., RUTA V., CADENE M., CHAIT B. and MACKINNON R., Nature, 423 (2003) 33.
- [5] LEE S.-Y., LEE A., CHEN J. and MACKINNON R., Nature, 102 (2005) 15441.
- [6] SCHMIDT D., CROSS S. R. and MACKINNON R., J. Mol. Biol., 390 (2009) 902.
- [7] MARMONT G., J. Cell Comp. Physiol., 34 (1949) 351.
- [8] KOCH C., Biophysics of Computation (Oxford University Press) 1999.
- [9] CHAIKIN P. and LUBENSKI T., Principles of Condensed Matter Physics (Cambridge University Press) 1995.
- [10] BUIJNSTERS F., FASOLINO A. and KATSNELSON M., Phys. Rev. Lett., 113 (2014) 217202.
- [11] KOLAR H., SPENCE J. and ALEXANDER H., Phys. Rev. Lett., 77 (1996) 4031.
- [12] ROTERMUND H., JAKUBITH S., VON OERTZEN A. and ERTL G., Phys. Rev. Lett., 66 (1991) 3083.
- [13] Loewenstein Y. and Sompolinsky H., *Nat. Neurosci.*, **6** (2003) 961.
- [14] CHARLES A., MERRILL J., DIRKSEN E. and SANDERSON M., Neuron, 6 (1991) 983.
- [15] WOLSZON L. R., REHDER V., KATER S. B. and MACAGNO E. R., J. Neurosci., 74 (1994) 3437.
- [16] WEISSMAN T. A., RIQUELME P. A., IVIC L., FLINT A. C. and KRIEGSTEIN A. R., Neuron, 43 (2004) 647.
- [17] MCNAMARA H., SALEGAME R., AL TANOURY Z., XU H., BEGUM S., ORTIZ G., POURQUIE O. and COHEN A. E., Nat. Phys., 16 (2020) 357.
- [18] HODGKIN A. L. and HUXLEY A. F., J. Physiol. (London), 117 (1952) 500.
- [19] FITZHUGH R., $Biophys.\ J.,\ {\bf 1}\ (1961)\ 445.$
- [20] NAGUMO J., ARIMOTO S. and YOSHIZAWA S., Proc. IRE, 50 (1962) 2061.
- [21] VASQUEZ H. G. and ZOCCHI G., Bioinspir. Biomim., 14 (2019) 016017.
- [22] ARIYARATNE A. and ZOCCHI G., Phys. Rev. E, 91 (2015) 032701.
- [23] VAN DER POL B., Philos. Mag., 2 (1926) 978.
- [24] Buijnsters F., Fasolino A. and Katsnelson M., Nature, 426 (2003) 812.
- [25] MORRIS C. and LECAR H., Biophys. J., 35 (1981) 193.
- [26] PI Z. and ZOCCHI G., arXiv:2012.00221 (2020).
- [27] VANAG V. K. and EPSTEIN I. R., Phys. Rev. Lett., 92 (2004) 128301.